Evidence of chemical short-range order in amorphous CuTi alloys produced by mechanical alloying

1992 J. Phys.: Condens. Matter 4 1635

(http://iopscience.iop.org/0953-8984/4/7/003)

J. Phys.: Condens. Matter 4 (1992) 1635–1645. Printed in the UK

Evidence of chemical short-range order in amorphous CuTi alloys produced by mechanical alloying

P K Ivison†, I Soletta‡, N Cowlam†, G Cocco‡, S Enzo§ and L Battezzati‖

† Department of Physics, University of Sheffield, Sheffield S3 7RH, UK
‡ Dipartimento di Chimica, Università di Sassari, via Vienna 2, 07100 Sassari, Italy
§ Dipartimento di Chimica Fisica, Università di Venezia Calle Larga, S Marta 2137, 30123 Venice, Italy
‖ Dipartimento di Chimica Inorganica, Chemica Fisica e Chimica dei Materiali, via P Guiria 9, 10125, Turin, Italy

Received 12 July 1991, in final form 29 October 1991

Abstract. Neutron and x-ray diffraction measurements have been made on a series of eight mechanically alloyed CuTi amorphous alloys having atomic compositions between 75 and 30 at.% copper. The neutron measurements have shown that the alloys have a small impurity of hydrogen, which is attributed to contamination of the parent titanium powder. After appropriate corrections, the structure factors for these alloys have been found to be broadly similar to those of both glassy and molten CuTi specimens. The radial distribution functions provide some evidence of detailed differences between the atomic-scale structures of the molten, glassy and mechanically alloyed samples, which will need to be confirmed by measurements on samples of higher purity. The possible influence of gaseous impurities on the MA process is discussed.

1. Introduction

Since the first detailed examination (Koch *et al* 1983) of amorphization by mechanical alloying (MA), many different examples have been found of alloys that undergo an 'amorphization reaction' or a 'solid-state reaction' by this means. Advantages of MA over more conventional techniques for the production of disordered materials, such as chill-block melt-spinning and vapour condensation, include the potential for producing bulk amorphous material and the ability to create amorphous structures over wide composition ranges.

Early–late transition metal alloys based on titanium or manganese are especially interesting in neutron scattering since these two nuclei exhibit resonant scattering. Unlike the usual s-wave potential scattering, resonant scattering shows no phase difference between incident and scattered neutron waves. As a consequence, these nuclei are assigned negative values of scattering amplitude ($b_{Ti} = -0.3438 \times 10^{-12}$ cm and $b_{Mn} = -0.373 \times 10^{-12}$ cm). There is then a strong contrast between the atomic species in a neutron-scattering experiment on a binary alloy based on titanium or manganese (a 'negative scatterer') and a normal, potential-scattering element, such as most of the

0953-8984/92/071635 + 12 $04.50

Table 1. The compositions and MA treatment time are given for the eight a-Cu_xTi_{100-x} alloys studied, together with the weighting terms for the Bhatia–Thornton (1970) and Faber–Ziman (1965) partial structure factors.

	Milling time (hours)	W_{NN}	$\frac{W_{CC}}{x(1-x)}$	W_{CuCu}	W_{CuTi}	W_{TiTi}
$Cu_{75}Ti_{25}$	16	0.514	0.486	1.37	−0.40	0.03
$Cu_{70}Ti_{30}$	16	0.427	0.573	1.52	−0.57	0.05
$Cu_{60}Ti_{40}$	16	0.266	0.734	2.00	−1.17	0.17
$Cu_{55}Ti_{45}$	16	0.196	0.804	2.43	−1.74	0.31
$Cu_{50}Ti_{50}$	16	0.132	0.868	3.17	−2.78	0.61
$Cu_{45}Ti_{55}$	16	0.079	0.921	4.64	−4.97	1.33
$Cu_{40}Ti_{60}$	25	0.036	0.964	8.52	−11.20	3.68
$Cu_{30}Ti_{70}$	16	1×10^{-4}	0.999	1.95×10^{3}	-3.98×10^{3}	2.03×10^{3}

other transition metals. This expedites the precise measurement of chemical short-range order (CSRO).

There is a well-established framework to describe CSRO in disordered materials, which illustrates very clearly the advantages of 'negative scattering'. The partial structure factors (PSFs) defined for a binary alloy A_xB_{1-x} by Bhatia and Thornton (1970) give, for neutrons,

$$S(Q) = (\langle b\rangle^2 S_{NN}(Q) + 2\Delta b\,\langle b\rangle\, S_{NC}(Q) + \Delta b^2\, S_{CC}(Q))/\langle b^2\rangle \qquad (1)$$

where b is the scattering amplitude

$$\langle b\rangle = xb_A + (1-x)b_B \qquad \langle b^2\rangle = xb_A^2 + (1-x)b_B^2 \qquad \Delta b = b_A - b_B$$

The number–number PSF $S_{NN}(Q)$ relates to variations in topological short-range order (TSRO) and the concentration–concentration PSF $S_{CC}(Q)$ to variations in CSRO. $S_{NC}(Q)$ is a size-effect PSF, which accounts, for example, for variations in CSRO stimulated by differences in atomic sizes of the constituents and for variations of TSRO stimulated by chemical affinities. The Fourier transforms of $S_{NN}(Q)$ and $S_{CC}(Q)$ give the familiar radial distribution function (RDF) $4\pi r^2\rho_{NN}(r)$ and the radial concentration function RCF $4\pi r^2\rho_{CC}(r)$ respectively.

If the scattering amplitudes b_A, b_B of the two alloy constituents have different signs, then Δb becomes large, promoting the visibility of CSRO at the expense of TSRO. If in addition the size difference between the alloy constituents is small and $S_{NC}(Q)$ can be neglected, (1) can be simplified to:

$$S(Q) \simeq W_{NN}S_{NN}(Q) + W_{CC}S_{CC}(Q)/x(1-x) \qquad (2)$$

Here

$$W_{NN} = \langle b\rangle^2/\langle b^2\rangle \qquad W_{CC} = x(1-x)\Delta b^2/\langle b^2\rangle = 1 - W_{NN}$$

are the weighting factors for $S_{NN}(Q)$ and $S_{CC}(Q)/x(1-x)$. Both of these latter terms have limiting values of unity. As $\langle b\rangle \to 0$ at the 'null matrix' composition, the total structure factor $S(Q)$ relates to CSRO effects alone; see table 1. At this point the alternative definition of the PSFs in terms of pair correlations, due to Faber and Ziman (1965),

$$S(Q) = [x^2b_A^2S_{AA}(Q) + 2x(1-x)b_Ab_BS_{AB}(Q) + (1-x)^2b_B^2S_{BB}(Q)]/\langle b\rangle^2 \qquad (3)$$

becomes unstable; see table 1. In addition, the weighting factor for $S_{AB}(Q)$ is negative

at all compositions, if either b_A or b_B is negative. It must be emphasized that the high visibility of CSRO resulting from 'negative scattering' nuclei does not occur with the other radiations (*x*-rays or electrons), so neutron scattering gives, in these circumstances, a sensitivity to CSRO that is unrivalled by any other technique.

The study of CSRO in amorphous CuTi alloys discussed in the present paper is particularly interesting, not just as a convenient example of a positive-scattering/negative-scattering combination ($b_{Cu} = 0.7718 \times 10^{-12}$ cm and $b_{Ti} = -0.3438 \times 10^{-12}$ cm) but also because their study (Cocco *et al* 1990) allows comparison to be made with the accumulated data on CuTi alloys in the glassy and liquid states. Since CuTi alloys, unlike NiTi, glass-form over a wide composition range, a convincing demonstration can be given (Sakata *et al* 1980, 1982) that the degree of CSRO present correlates with the glass stability. Experiments on liquid CuTi alloys have also confirmed that this CSRO exists in the melt (Sakata *et al* 1981, He Fenglai *et al* 1986), where it is presumably a precursor for what is observed after vitrification in the glassy phase.

The factors that influence amorphization reactions and their relative importance are much less well known than, say, those for vitrification by the melt-spinning process. The principal aim of the present work was therefore to investigate the role of CSRO in the a-CuTi amorphization reaction.

2. Sample preparation and experimental procedure

Appropriate amounts of Cu (ALFA-200 mesh, 4N quoted purity) and Ti (VENTRON-325 mesh, 2N quoted purity) powders were milled in a hardened steel vial using a Spex Mixer-Mill (model 8000). The ball-to-powder weight ratio was 8.3 with $\frac{1}{2}$" (12.5 mm) balls. Milling was carried out under an argon atmosphere to prevent oxidation. Eight samples were prepared, having compositions of 30–75 at.% copper. Table 1 shows the sample compositions and milling times. Note that the 'null matrix' composition $Cu_{30.8}Ti_{69.2}$ is just within this range, although it is just outside the glass-forming range (Sakata *et al* 1982). The samples were examined with x-rays immediately after the MA treatment in order to confirm their structure. A short scan of 3–4 h covering the first broad diffraction maximum was employed, using a Siemens D500 diffractometer with CuK_α radiation.

Neutron diffraction measurements were made on these eight samples, together with a specimen of the parent powders mixed in the proportions $Cu_{40}Ti_{60}$, using the D20 diffractometer at the Institut Laue–Langevin, Grenoble. A copper monochromator giving an incident neutron wavelength $\lambda = 0.94$ Å was used. The samples were examined in thin-walled vanadium tubes (external diameter 7 mm) filled to a depth of approximately 15 mm and placed at the centre of an evacuated cloche. A typical scan was made by moving the multidetector (whose elements were spaced at intervals of 0.10°) in steps of 3° from 4° to 142° with a count time of order 200 s per step. This gave a usable angular range in 2θ of 4° to 155° and a scan time of approximately 3 h. A preliminary scan was made using a silicon standard in order to calibrate wavelength and calculate the zero-offset in 2θ. Background and calibration scans were made using the empty vanadium tube and a 7 mm vanadium rod, respectively.

3. Data analysis

The multidetector data were corrected for zero-offset and individual detector efficiency, and were regrouped as intensity versus scattering angle 2θ. The diffraction patterns for

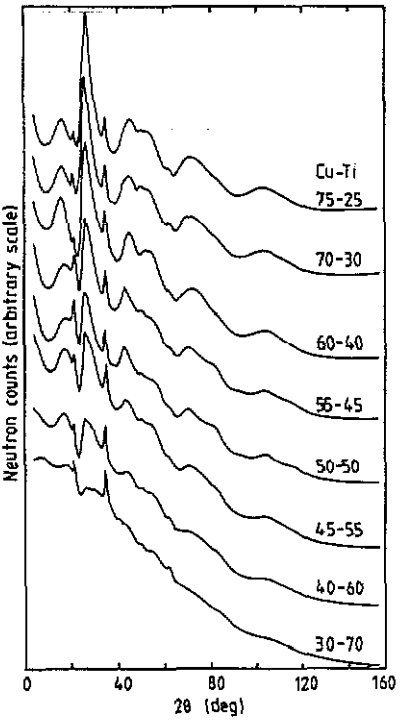

Figure 1. Neutron diffraction patterns of the eight a-Cu_xTi_{100-x} alloys. The large sloping background level is indicative of hydrogen contamination in the samples. 2θ is the scattering angle.

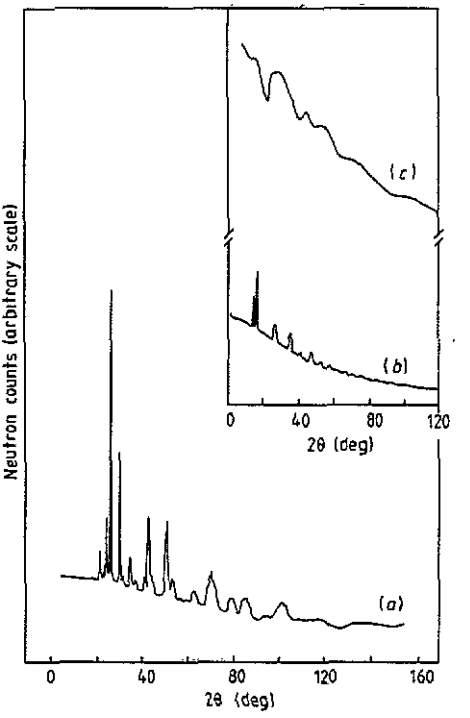

Figure 2. (*a*) Neutron diffraction pattern of the parent copper and (hydrogen-contaminated) titanium crystalline powders mixed in the ratio $Cu_{40}Ti_{60}$. A correction for hydrogen inelastic scattering was obtained from this pattern. (*b*) The equivalent result from crystallic $TbH_{1.6}$ after Chieux *et al* (1984). (*c*) The diffraction pattern of a deliberately hydrogenated $(Cu_{50}T_{50})$–$H_{0.15}$ metallic glass (after Rodmacq *et al* 1985), for comparison with figure 1.

the eight samples are shown in figure 1. Each pattern shows a large fall in intensity as a function of scattering angle. This behaviour is typical of scattering from materials containing hydrogen. Hydrogen has the largest value of incoherent neutron-scattering cross-section of all the elements, so its presence in the sample, even in small quantities, is easily noticed. The scattered intensity is not only high but has a characteristic angular dependence, owing to departure from the so-called 'static approximation' (Placzek 1952), which is, of course, largest for light atoms such as hydrogen. Evidence for the correctness of this interpretation is provided by a comparison with the neutron diffraction patterns of deliberately hydrogenated CuTi metallic glass ribbons, studied by Rodmacq *et al* (1985); see figure 2(*c*). Furthermore, the small Bragg peaks seen in the individual patterns of figure 1 can be identified with the (111) and (220) Bragg reflections from crystalline TiH_2 (Sidhu *et al* 1956). These small Bragg peaks were removed, using their calculated intensities as a reference before any further analysis was made. It should be emphasized that x-ray experiments are not particularly sensitive to hydrogen contamination below about 5% (Cocco 1991) on account of the weakness of the x-ray scattering from the single electron of hydrogen.

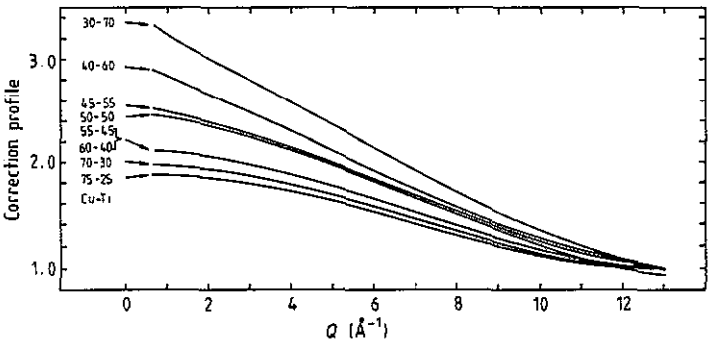

Figure 3. Correction curves for the inelastic scattering from the hydrogen atoms, as deduced for the eight alloy compositions Cu_xTi_{100-x} as a function of Q, the scattering vector. Note the suppressed zero on the ordinate and the sequence of the curves, which is the reverse of that in figure 1, with the highest titanium concentration at the top.

The diffraction patterns of figure 1 need to be corrected for the background scattering, the vanadium sample containers and the hydrogen in the specimens. They then need to be normalized and finally to be replotted in equal increments of Q in order to obtain the total structure factor $S(Q)$. In the absence of a precise knowledge of the metal–hydrogen interactions and their dynamics, a semi-empirical correction must be used, of which several exist. The procedure applied by Chieux *et al* (1984) to the case of a hydrogen-contaminated TbCu amorphous alloy consists of using the background scattering intensity from an equivalent hydrogen-bearing crystalline phase. Figure 2(*a*) shows the diffraction pattern from D20 for the parent crystalline powders $Cu_{40}Ti_{60}$, from which a correction curve was obtained by first smoothing and then curve-fitting the background, using in this case a fourth-order polynomial. The resulting profile was found to be very similar to the correction obtained by Chieux *et al* (1984), shown in figure 2(*b*). The correction was then applied, with a simple scaling factor derived from the neutron count rates, to the diffraction patterns of the other CuTi alloys, where it was found to work well for specimens with less than 50% titanium, but was less successful for the three titanium-rich alloys. This confirms that a proper correction depends on both the concentration and the dynamics of the hydrogen present. For these latter alloys, the procedure of Rodmacq *et al* (1985) was used, namely choosing a polynomial such that the resultant data oscillated about a horizontal line. Figure 3 shows a superposition of all the hydrogen correction profiles, which have a regular increase in magnitude and gradient. Indeed, independent evidence from work on Zr_3Rh–H amorphous hydrides has shown that these and other suggested corrections have remarkably similar form (Mohammed 1991).

The last stage in obtaining $S(Q)$ was to normalize the corrected intensity distribution. It did not appear to be appropriate to attempt a vanadium normalization in view of the arbitrary corrections for the hydrogen scattering, so an $I(0)$–$I(\infty)$ self-normalization method, as discussed by Enderby (1968), was used. The levels $I(0)$, $I(\infty)$ were chosen with the total scattering $\langle b^2 \rangle$ in mind. There was some uncertainty in the low-Q limit $I(0)$, caused by the increase in scattering in this region, which will be discussed later; the initial choices of the $I(0)$, $I(\infty)$ levels were adjusted slightly in order to minimize the spurious ripples in the resulting Fourier transform. This technique, which does not alter the features of the resulting RDF, has been discussed by Lorch (1969) as the 'zero ripple'

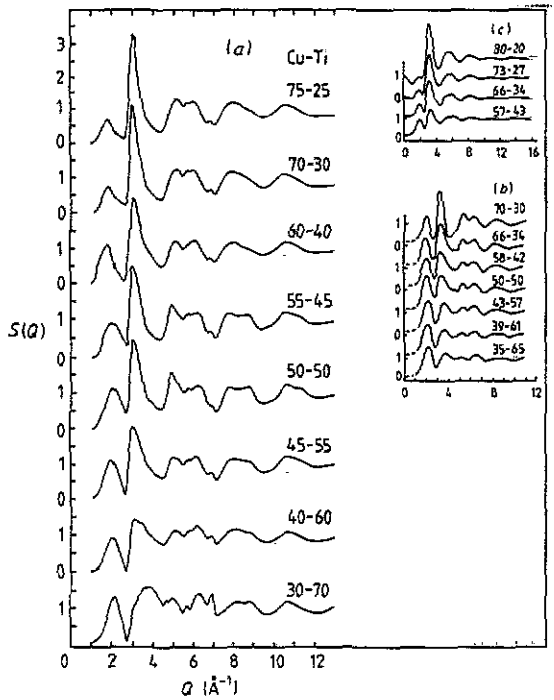

Figure 4. (*a*) Total-structure factors $S(Q)$ for the eight a-Cu_xTi_{100-x} alloys. (*b*) The equivalent curves for glassy Cu_xTi_{100-x} alloys and (*c*) the equivalent curves for molten Cu_xTi_{100-x} alloys. *Q is the scattering vector.*

method. The resulting total structure factors $S(Q)$ are shown in figure 4 and all details of the correction and normalization processes have been given elsewhere (Ivison 1991).

4. Total structure factors for a-CuTi alloys

The most encouraging features of the curves shown in figure 4 are their regular variation with composition and their overall similarity with the equivalent curves obtained by neutron diffraction for CuTi alloys in the glassy state (Sakata *et al* 1982) and liquid state (He Fenglai *et al* 1986). These latter curves are shown as inserts to the figure. The $S(Q)$ for mechanically alloyed $Cu_{75}Ti_{25}$ has a form very similar to that for most metallic alloy glasses, with an intense first peak at $Q_{FP} \simeq 3.1$ Å^{-1}, a second peak with a shoulder, and subsequent oscillations out to Q_{max}. However, as the alloy concentration changes, the small pre-peak in $S(Q)$ of $Cu_{75}Ti_{25}$ at $Q_{pp} \simeq 1.9$ Å^{-1} grows as the first peak diminishes, *until they are comparable in magnitude for the* $Cu_{30}Ti_{70}$ *specimen.*

While it is true that *all* the features of $S(Q)$ transform to give the shape of $G(r)$, it is generally accepted that strong features (positive or negative) in $S(Q)$ at a given Q value (Q_1) can be associated with resulting features in $G(r)$ at r_1, say, via the relation $r_1 = \frac{n}{4}2\pi/Q_1$, where $\frac{n}{4}$ represents the first term of the series $\frac{5}{4}$, $\frac{9}{4}$, $\frac{13}{4}$, ... (See Klug and Alexander (1974) p 848 and Cargill (1975) p 269 for a practical example.) Using this relation and the experience gained from CuTi glasses and liquids, the first peak in $S(Q)$ can be associated with the dominant first-neighbour correlations $r_1 = \frac{5}{4}2\pi/Q_{FP} \simeq 2.5$ Å,

and the pre-peak is associated with like-atom correlations at the second-neighbour distance $r_2 = \frac{5}{4}.2\pi/Q_{pp} \simeq 4.1$ Å. The pre-peak is therefore equivalent to a superlattice peak in the diffraction pattern of a crystalline material and is indicative of true short-range order, unlike first neighbours and like-atom second neighbours. This identification is aided by the fact that in the Faber–Ziman definition of the PSFs, the like-atom contributions to $S(Q)$, $S_{CuCu}(Q)$ and $S_{TiTi}(Q)$ are positive because they depend on the square of the scattering lengths, while the unlike atom contributions $S_{CuTi}(Q)$ are always negative on account of the negative value of b_{Ti}.

A comparison of the structure factors (figure 4) shows that the pre-peak is never as well developed for the MA specimens as for the glasses. However, the first peak in $S(Q)$ is quite sharp for those MA specimens with the highest copper concentrations. This suggests that their topological structures are probably quite well developed but the degree of CSRO is smaller. Comparison of $S(Q)$ for the liquid and MA samples is restricted to the copper-rich alloys, which are more accessible in the liquid state. While the peak ratios are closer for these two states, inspection of figure 4 shows that this is due to the fact that the first peak in $S(Q)$ is smaller for the liquid state. Thus TSRO is, as expected, reduced at high temperature in the liquid alloys but CSRO still remains significant.

A study of the extent of CSRO present in these samples would require, at minimum, a separation of the total $S(Q)$ into at least $S_{NN}(Q)$ and $S_{CC}(Q)$ by means of a combination of x-ray and neutron data. However, while the weighting factors W_{NN} and W_{CC} of table 1 show that $S_{NN}(Q)$ can almost be neglected for the titanium-rich samples, the empirical corrections applied to the data above suggest that even this approach should be used with caution. Previously (Ivison *et al* 1991) we have chosen to use the relative heights of the pre-peak and main peak in $S(Q)$ as a simple indication of the degree of CSRO present. However, in retrospect this may be confusing because the increase of this ratio with composition is in the reverse sense to the increase of the Cowley CSRO parameter with composition. This can be seen from a comparison of figure 3 from Ivison *et al* (1991) with figure 5 from He Fenglai *et al* (1986). A better measure of the CSRO present is therefore probably given by the normalized ratio: R_N = (Height of pre-peak/W_{CC})/(Height of main peak/W_{NN}).

This ratio illustrates the point that the existence of the CSRO and its visibility in the experiment are equally important. The ratio R_N is plotted in figure 5 as a function of composition for the present MA samples (5(*b*)) and for the glassy (5(*a*)) and molten alloy states (5(*c*)) (Sakata *et al* 1982 and He Fenglai *et al* 1986 respectively). The values of the ratio R_N for the MA samples are smaller than those for the glassy state and about the same as those for the molten alloys. The variation of R_N with composition for the MA samples is intermediate between the other two states.

5. Real space structures of a-CuTi alloys

The Fourier transform of a total-structure factor $S(Q)$ is normally presented as a radial distribution function (RDF), $4\pi r^2\rho(r)$. Just as $S(Q)$ contained three PSFs so the RDF also contains three separate density functions. Table 1 shows that for the copper-rich alloys $S(Q)$ contains roughly equal contributions from $S_{NN}(Q)$ and $S_{CC}(Q)$, so it is convenient to present their Fourier transform as an RDF. However, as the titanium concentration increases, table 1, so the weighting term for $S_{CC}(Q)$ becomes dominant (and the Faber–Ziman weighting factors also diverge). Thus for these latter alloys it is sensible to present the Fourier transform as an RCF, $4\pi r^2\rho_{cc}(r)$. The RCF is defined without the parabolic

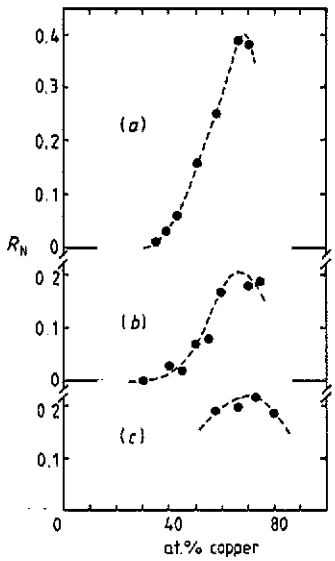

Figure 5. Normalized peak ratio R_N (defined in the text) plotted as a function of composition: (*b*) for the present MA samples, (*a*) for glassy Cu_xTi_{100-x} and (*c*) for molten Cu_xTi_{100-x}.

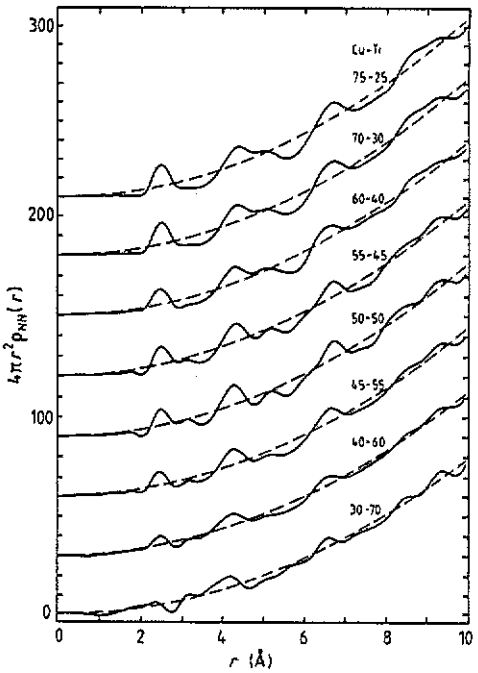

Figure 6. Radial distribution functions (RDFs) for the a-Cu_xTi_{100-x} alloys, derived from the total structure factors shown in figure 4.

background and oscillates about zero in such a way that positive features represent like-atom (Cu–Cu, Ti–Ti) correlations and negative ones unlike-atom (Cu–Ti, Ti–Cu) correlations. The Fourier transform for $Cu_{30}Ti_{70}$ actually gives the RCF, since $W_{cc}/x(1-x) = 0.999$, and for the other titanium-rich alloys it provides a reasonable approximation.

Figure 6 shows that there is a regular variation of the RDF with composition, following that of the structure factors from which they are derived. Starting from the $Cu_{75}Ti_{25}$ alloy, the first peak at $r \simeq 2.5$ Å, which remains in about the same position for all the alloys, can certainly be associated with Cu–Cu correlations. Equally the second feature, which emerges in the equiatomic region at about 3 Å, is probably associated with Ti–Ti pairs (see table 1). In the RCFs a substantial positive peak occurs at $r \simeq 2.5$ Å for copper-rich alloys which must be from Cu–Cu first neighbours. It is reduced in size for the $Cu_{40}Ti_{60}$ alloy but it is only for $Cu_{30}Ti_{70}$, which is near the null-matrix composition, that a strong negative peak occurs, at $r \simeq 2.8$ Å. This is from Cu–Ti unlike pairs and is close to the sum of the Goldschmidt radii of copper and titanium, 2.75 Å. Just as the area under the first peak of the RDF gives the coordination number n_1, so the integral of the RCF over the same range of radial distances gives $n_1\alpha_1$ where α_1 is the Cowley short-range order parameter for the first shell of atoms (Cowley 1950). Thus inspection of figure 7 shows that only the $Cu_{30}Ti_{70}$ alloy appears to have a negative value of α_1, which is the characteristic evidence of true short-range order for all the CuTi glasses (Sakata *et al* 1982) and CuTi molten alloys (He Fenglai *et al* 1986).

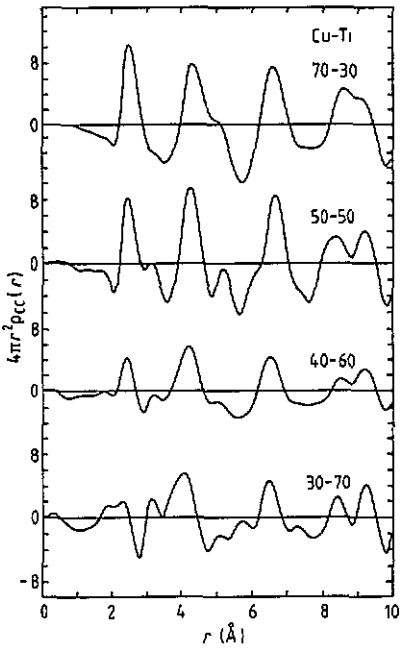

Figure 7. RDFs given in figure 6, presented for four of the a-Cu_xTi_{100-x} alloys in the form of radial concentration functions, $4\pi r^2\rho_{cc}(r)$, to show their evolution with composition.

It is difficult to know whether this somewhat unexpected observation will be sustained when a proper derivation of $S_{NN}(Q)$ and $S_{CC}(Q)$ is made in the future. It must be recalled, however, that the evidence for CSRO in the glassy and liquid CuTi alloys does not rest on the presence of a large pre-peak in $S(Q)$ for titanium-rich alloys but rather on the presence and magnitude of the smaller pre-peak in the copper-rich alloys.

It is also possible that the present observation has been influenced by the hydrogen contamination in the samples, estimates of which were made by DSC measurements. A peak in the DSC trace of the contaminated samples could be clearly associated with the evolution of hydrogen. By careful control of the heating rate and by comparison with standard samples of TiH_2, it was estimated that the hydrogen impurity in the parent titanium powder was approximately 15%. This reduces to contaminations of between 4 and 10 at.% for the actual CuTi specimens. To estimate the influence of this on the total $S(Q)$ it is necessary to calculate the weighting terms for the six PSFs of the ternary system CuTi–H. However, since hydrogen, like titanium, has a negative scattering amplitude, $b_H = -0.374 \times 10^{-12}$ cm, the problems of negative contributions to $S(Q)$ and the divergence of the weighting factors as $\langle b\rangle \to 0$ occur for CuTi–H, as for CuTi alloys. We postulate therefore that since hydrogen/metal ratios of order unity can be obtained in the CuTi–H system (Grzeta *et al* 1985), concentrations of about 5% hydrogen probably do not play a significant role in determining the structures of the amorphous matrix of the CuTi alloys examined here. However, it is clear that the preference of hydrogen for Ti_4H tetrahedral sites could stimulate segregation by normal diffusion. Such segregation would also result in the appearance of strong forward scattering at small Q values. This is, in fact, observed for these CuTi and other alloys produced by MA (Fukunaga *et al* 1990a, 1990b), but is more likely to result from inhomogeneous strain fields associated with the high-energy MA process. On an atomic scale, the formation of Ti_4H tetrahedra within a disordered specimen should lead to the appearance of stretched Ti–Ti neighbour

bonds at $r \approx 3.14$ Å, as observed in crystalline TiH_2 (Sidhu *et al* 1956). However, it is unlikely that this could account for the feature in the RDFs of the equiatomic CuTi alloys seen in figure 6 at the hydrogen concentrations involved.

6. Conclusions

Neutron and x-ray diffraction measurements have been made on a series of eight mechanically alloyed CuTi amorphous alloys having at.% compositions between 75 and 30 at.% copper.

The neutron measurements have confirmed that the alloys have amorphous structures, but also that they were contaminated with between 4 and 10 at.% hydrogen. A series of corrections have been made to the neutron diffraction patterns to enable the structure factors $S(Q)$ to be obtained. The similarity of these $S(Q)$ to those of CuTi metallic glasses and CuTi molten alloys studied by us in the past indicates that the disordered structures of all three phases may be broadly similar. The important pre-peak present in the $S(Q)$ of the MA specimens illustrates that CSRO exists in the samples, and its intensity and variation with composition appear to be intermediate between those of the glassy and molten states. The real space structures derived from the Fourier transform of the $S(Q)$ also appear to lack the strong Cu–Ti first-neighbour correlation seen in the other two phases.

The detection of the hydrogen impurity in the specimens, which was not suspected from the routine x-ray examination, has illustrated a long-established advantage of neutron scattering in the detection of light atoms, albeit through the *incoherent* scattering from the hydrogen. This hydrogen impurity clearly results from the use of contaminated titanium powder in the MA process. We are aware of the qualitative nature of their results in view of the arbitrary corrections for the hydrogen scattering that had to be applied, so the results are presented as being of general interest in the field of amorphization by MA. We suggest that gaseous contamination is an important factor that must always be taken into account in the MA process, for three reasons. First, MA invariably uses active metals such as titanium, zirconium and hafnium, in the form of finely divided powders having a high surface area/volume ratio. Second, suppliers of even spectroscopically pure materials do not always specify gaseous impurities with the same thoroughness as metallic impurities. Third, if scientific studies lead eventually to the use of MA powders on an industrial scale, the levels of contaminants will invariably be higher than in the present case and their role in the amorphization reaction will have to be taken into account.

Further x-ray and neutron scattering measurements are in progress to determine the static and dynamic properties of the dissolved hydrogen in these amorphous metals produced by the MA route. Measurements of CSRO are also in hand using materials of improved purity.

Acknowledgments

This work has been supported by ENEA contract 3965 and CNR contract 89.00605.69. The collaboration between Professor Cocco and Dr Cowlam is supported by a CNR/Royal Society Travel Grant. The neutron scattering measurements were performed with the support of the Science and Engineering Research Council and the help of Dr P Convert

at ILL, Grenoble. PKI acknowledges the support of an SERC studentship. A brief account of these measurements has been presented at the 7th International Conference on Rapidly Quenched Metals, Stockholm, 1990 (Ivison *et al* 1991).

References

Bhatia A B and Thornton D E 1970 *Phys. Rev.* B **2** 3004–12
Cargill G S 1975 *Solid State Phys.* **30** 227–320 (New York: Academic)
Chieux P, de Kouchkovsky R and Boucher B 1984 *J. Phys. F: Met. Phys.* **14** 2239–57
Cocco G 1991 *Proc. Int. Symp. Mech. Alloy (Kyoto, Japan)* at press
Cocco G, Soletta I, Enzo S, Magini M and Cowlam N 1990 *J. Physique Coll.* **C4** 181–7
Cowley J M 1950 *Phys. Rev.* **77** 667–75
Enderby J E 1963 *Physics of Simple Liquids* ed H N V Temperley *et al* (Amsterdam: North Holland) p 623
Faber T E and Ziman J M 1965 *Phil. Mag.* **11** 153–73
Fukunaga T, Nakamura K, Suzuki K and Mizutani U 1990a *J. Non-Cryst. Solids* **117 + 8** 700–3
Fukunaga T, Homma Y, Misawa M and Suzuki K 1990b *J. Non-Cryst. Solids* **117 + 8** 721–4
Grzeta B, Dini K, Cowlam N and Davies H A 1985 *J. Phys. F: Met. Phys.* **15** 2069–83
He Fenglai, Cowlam N, Carr G E and Suck J B 1986 *Phys. Chem. Liq.* **16** 99–112
Ivison P K 1991 *PhD thesis* University of Sheffield
Ivison P K, Cowlam N, Soletta I, Cocco G, Enzo S and Battezzati L 1991 *Mater. Sci. Eng.* **A134** 859–62
Klug H P and Alexander L E 1974 *X-ray Diffraction Procedures* (London: Wiley)
Koch C C, Cavin O B, McKarney C G and Scarbrough J O 1983 *Appl. Phys. Lett.* **43** 1017–235
Lorch E A 1969 *J. Phys. C: Solid State Phys.* **2** 229–37
Mohammed A A 1991 *PhD Thesis* University of Sheffield
Placzek G 1952 *Phys. Rev.* **86** 377–88
Rodmacq B, Mangin P L and Chamberod A 1985 *J. Phys. F: Met. Phys.* **15** 2259–72
Sakata M, Cowlam N and Davies H A 1980 *J. Physique* **8** 190–3
Sakata M, Cowlam N and Davies H A 1981 *J. Phys. F: Met. Phys.* **11** L157–62
Sakata M, Cowlam N and Davies H A 1982 *Proc. 4th Int. Conf. Rapidly Quenched Metals* **1** 327–9
Sidhu S S, Heaton Le R and Zauberis D D 1956 *Acta Crystallogr.* **9** 607–14